



Aberystwyth University

Solar Wind Speed Inferred from Cometary Plasma Tails using Observations from STEREO HI-1

Clover, John M.; Jackson, Bernard V.; Buffington, Andrew; Hick, P. Paul; Bisi, Mario M.

Published in:
Astrophysical Journal

DOI:
[10.1088/0004-637X/713/1/394](https://doi.org/10.1088/0004-637X/713/1/394)

Publication date:
2010

Citation for published version (APA):

Clover, J. M., Jackson, B. V., Buffington, A., Hick, P. P., & Bisi, M. M. (2010). Solar Wind Speed Inferred from Cometary Plasma Tails using Observations from STEREO HI-1. *Astrophysical Journal*, 713(1), 394-397.
<https://doi.org/10.1088/0004-637X/713/1/394>

General rights

Copyright and moral rights for the publications made accessible in the Aberystwyth Research Portal (the Institutional Repository) are retained by the authors and/or other copyright owners and it is a condition of accessing publications that users recognise and abide by the legal requirements associated with these rights.

- Users may download and print one copy of any publication from the Aberystwyth Research Portal for the purpose of private study or research.
- You may not further distribute the material or use it for any profit-making activity or commercial gain
- You may freely distribute the URL identifying the publication in the Aberystwyth Research Portal

Take down policy

If you believe that this document breaches copyright please contact us providing details, and we will remove access to the work immediately and investigate your claim.

tel: +44 1970 62 2400
email: is@aber.ac.uk

SOLAR WIND SPEED INFERRED FROM COMETARY PLASMA TAILS USING OBSERVATIONS FROM *STEREO* HI-1

JOHN M. CLOVER^{1,2}, BERNARD V. JACKSON^{1,2}, ANDREW BUFFINGTON^{1,2}, P. PAUL HICK^{1,2}, AND MARIO M. BISI^{1,2}

¹ Center for Astrophysics and Space Sciences, University of California, San Diego, 9500 Gilman Drive 0424, La Jolla, CA 92093-0424, USA; jclover@ucsd.edu, bjackson@ucsd.edu, abuffington@ucsd.edu, pphick@ucsd.edu, mmbisi@ucsd.edu

² Institute of Mathematical and Physical Sciences, Aberystwyth University, Penglais Campus, Aberystwyth, Ceredigion, SY23 3BZ, Wales, UK
 Received 2010 January 22; accepted 2010 February 26; published 2010 March 22

ABSTRACT

The high temporal and spatial resolution of heliospheric white-light imagers enables us to measure the propagation of plasma tails of bright comets as they travel through the interplanetary medium. Plasma tails of comets have been recognized for many years as natural probes of the solar wind. Using a new technique developed at the University of California, San Diego to measure the radial motion of the plasma tails, we measure the ambient solar wind speed, for the first time in situ at comets 2P/Encke and 96P/Machholz. We determine the enhanced solar wind speeds during an interplanetary coronal mass ejection encounter with 2P/Encke and compare these to previously modeled values, and also present solar wind speeds covering a range of latitudes for 96P/Machholz. We here apply this technique using images from the Sun–Earth Connection Coronal and Heliospheric Investigation Heliospheric Imagers (HI-1) on board the *Solar TERrestrial Relations Observatory-Ahead* spacecraft.

Key words: comets: individual (2P/Encke, 96P/Machholz) – solar wind – Sun: coronal mass ejections (CMEs) – techniques: radial velocities

1. INTRODUCTION

Comet observations have long been used to infer the nature of the solar wind (Biermann 1951; Parker 1958). The present authors used data from the Solar Mass Ejection Imager (SMEI; Eyles et al. 2003; Jackson et al. 2004) instrument to measure the solar wind speed, by tracking the propagation of the plasma tails of comets (Buffington et al. 2008). This analysis concluded that the “kinks” visible in these tails extending over great angular distances are frequently caused by varying solar wind speed at the location of the comet nucleus and manifest in white-light images as the comet plasma propagates radially outward. Also, these measurements indicate that the plasma visible a great distance ($\sim 10^6$ km) from the nucleus of the comet has become entrained in the solar wind.

This paper applies the technique used in that earlier analysis, to data from the Sun–Earth Connection Coronal and Heliospheric Investigation (SECCHI; Howard et al. 2000, 2008) Heliospheric Imager-1 (HI-1; Socker et al. 2000) on board the *Solar TERrestrial Relations Observatory-Ahead* (*STEREO-A*) spacecraft (Kaiser 2005; Kaiser et al. 2008). The fine angular resolution of these data, for two comets orbiting close to the Sun, provides a new application for the above technique. In particular, we highlight a comet plasma–tail interaction with an interplanetary coronal mass ejection (ICME) and provide measurements of the solar wind speed spanning a significant range of solar latitudes.

2. OBSERVATIONS

The HI-1 instrument observes heliospheric structures in white light, over a $20^\circ \times 20^\circ$ field of view centered 14° from the Sun. HI-1 images are made by combining many short exposures from a 1024×1024 (after 2×2 binning) CCD detector into 40 minute summed images (Eyles et al. 2009). These provide a higher temporal and spatial resolution than the 102 minute SMEI near-all-sky maps, but cover a smaller region of the sky. Plasma tails of the comets in the SMEI analysis are visible up

to 90° from the nucleus on the plane of the sky, which can cover a distance of up to 0.5 AU. The plasma tails of the comets observed in the HI-1A images used in the present analysis are visible over an angular distance of about 10° and extend up to 0.1 AU from the nucleus.

2.1. SMEI

In the previous analysis (Buffington et al. 2008), to measure the radial speed of the plasma tails of comets C/2001 Q4 (NEAT) and C/2004 T7 (LINEAR), equal-angle fish-eye sky maps were constructed from individual SMEI sky maps with stars and background removed (e.g., Hick et al. 2007). Ephemerides obtained from the Minor Planet & Comet Ephemeris Service³ provide the comet-nucleus location in three-dimensional space. A straight line from the Sun to the comet nucleus is projected onto the Sun-centered fisheye sky map as viewed from Earth (Figure 1, top panel, black line). This original projected line remains fixed in space and time as the sequence of SMEI images steps forward in time and the comet moves in its orbit providing a new radial (white line). Features appearing to cross the black line seen in later images are measured and their elongation versus time determined. The elongation is then converted into a radial distance along the Sun–comet line from the temporal and spatial locations of the comet nucleus at the time when the black line is first projected (see Figure 1, bottom image).

This process is repeated for each SMEI sky map where sufficient data are available. With the radial distance of the plasma from the original comet nucleus location known on successive images, the plasma-tail distance from the nucleus divided by elapsed time provides a radial speed of the solar wind. For each measurement, this indicates the solar wind speed past the comet nucleus assuming no further speed change between the nucleus and the measurement location. Figure 2 shows these speed measurements as a contour plot with the position of the comet nucleus along its orbital path (horizontal axis) versus

³ <http://www.cfa.harvard.edu/iau/MPEph/MPEph.html>

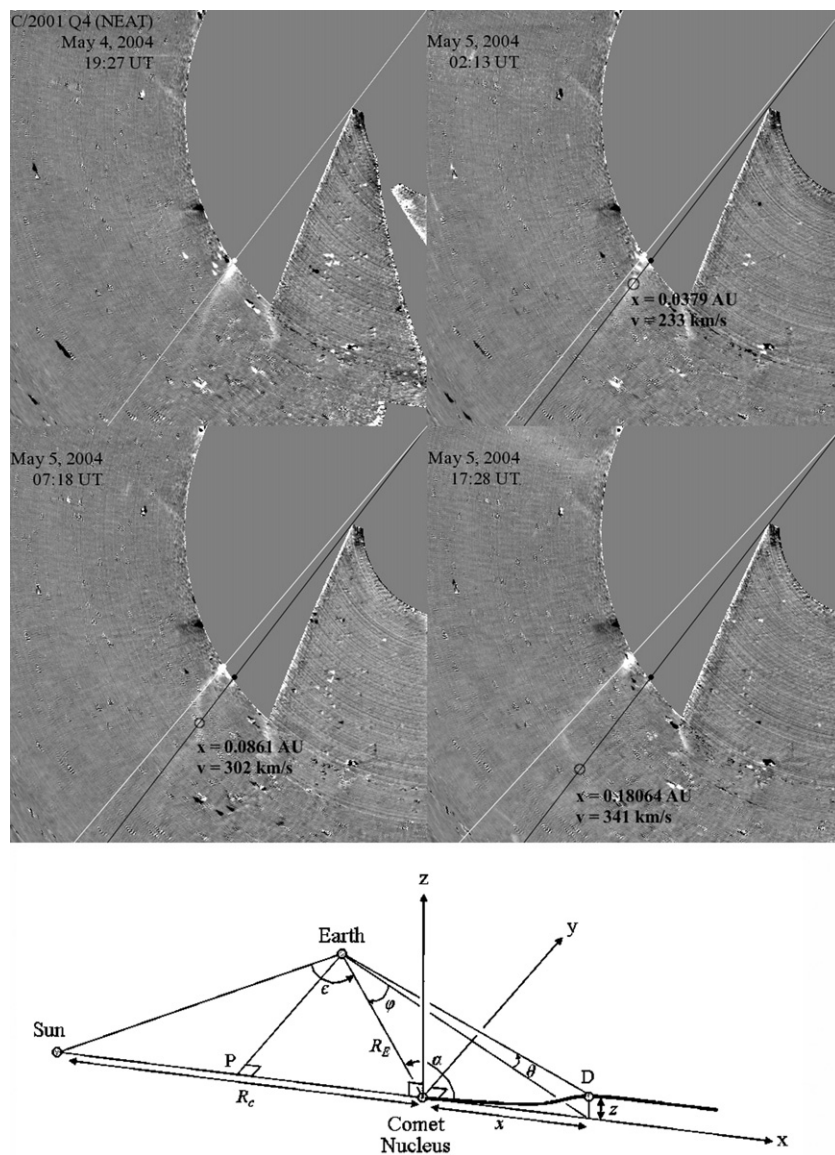


Figure 1. Top: graphical representation of measurements made of NEAT with a $50^\circ \times 50^\circ$ section of a SMEI fisheye sky map. Bottom: schematic of the geometry used to convert the measured elongation ϕ in an equal angle projection to a distance along the Sun-comet line x . This figure and the next are from Buffington et al. (2008).

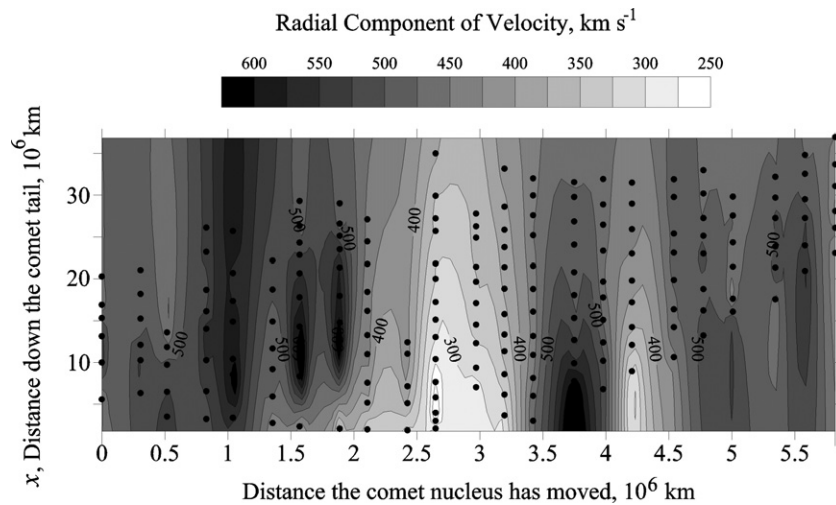


Figure 2. NEAT radial velocity contour, beginning 2004 May 4 at 02:31 UT through 2004 May 5 at 15:46 UT using measurements from SMEI sky maps. The Buffington et al. (2008) article's time range for this figure, in both the text and the caption for Figure 6, is in error and should instead be these values.

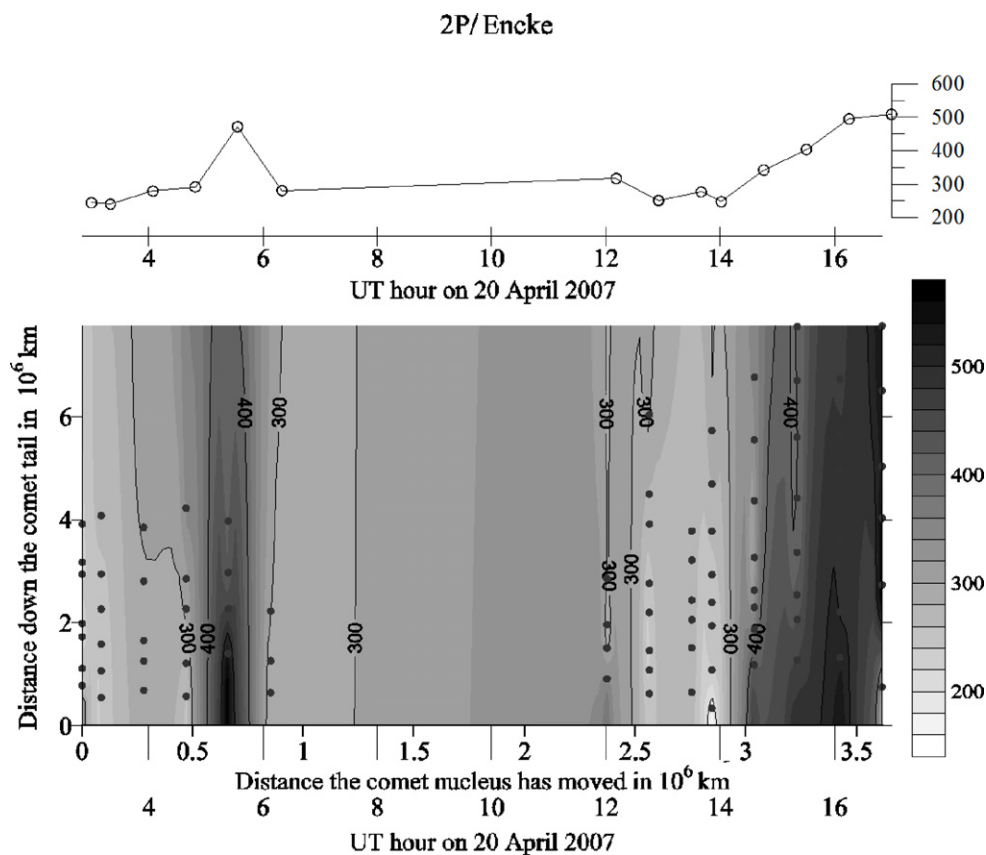


Figure 3. Radial velocity measurements of comet 2P/Encke. Bottom: velocity contours in km s^{-1} , beginning 2007 April 20 at 02:50 UT, using measurements from HI-1A images. Speed data are unavailable between 6 and 12 h UT, and after 16:50 UT. Top: average speed in km s^{-1} , of each vertical column of radial measurements in the bottom panel.

distance down the Sun–comet line (vertical axis); both are in units of 10^6 km. The dots are the measurement locations along each projected radial line. The large low-velocity region at 2.5×10^6 km on the horizontal axis in Figure 2 coincides with the onset of a large “kink” in the plasma tail of the comet. This low-velocity feature is believed to be related to a solar wind transient (Kuchar et al. 2008).

2.2 STEREO HI-1A

In 2007 April, two comets were visible in the *STEREO* HI-1A field of view: 2P/Encke, with an orbit slightly inclined from the ecliptic plane, moved toward *STEREO*-A, and 96P/Machholz, on a highly inclined orbital plane nearer to the Sun, moved from south to north across the field of view. During this time Encke underwent a dramatic plasma tail disconnection caused by an ICME (Vourlidas et al. 2007). Our measurements (Figure 3) indicate that the plasma picked up by the solar wind when the bright portion of the ICME passes has an average radial velocity of about 500 km s^{-1} , higher than the ambient solar wind speed and in agreement with the findings of Vourlidas et al. (2007). The data gaps between 6 and 12 UT contained too few points to be reliable; we measure no speed for plasma picked up near the nucleus after 16:50 UT, immediately following the high velocity region, because of the complete disconnection of the plasma tail.

Prior to this sudden disconnection of 2P/Encke’s plasma tail, HI-1A also observed 96P/Machholz. During this time, the comet passed as close as 0.14 AU from the Sun and through a wide range of heliographic latitudes. Speed measurements over this time provide detailed information about the latitudinal variation of the solar wind speeds close to the Sun.

Contours in Figure 4 show smooth transitions through regions of high-speed solar wind at about -25° , -22° , -20° , and -18° heliographic latitude. Averages of all the radial velocity measurements at a given time (upper panel) somewhat smooth this out, but show that the speed undergoes a gradual decrease as Machholz passes between -18° and -14° heliographic latitude and approaches the solar equator.

3. DISCUSSION AND CONCLUSIONS

The present work employs our previously developed technique using SMEI data, to determine solar wind speeds with *STEREO* HI-1A data, by measuring the radial propagation of comet plasma picked up by the solar wind. This method enables opportunistic measurement of solar wind speeds over large areas of space when comets are present and active, thus probing a wide range of latitudes and distances that otherwise are not readily accessible for direct in situ measurements by spacecraft. We also present measurements of the solar wind speeds at low heliographic latitudes before Machholz approaches perihelion. The decrease in the speed from about 550 km s^{-1} to 450 km s^{-1} at about 03:30 UT is associated with a region of greater brightness observed in HI-1A. The solar wind speeds at these locations are generally much higher than those encountered by Encke, but unlike Encke, Machholz does not appear to undergo any disconnection of its plasma tail. When variation in the ambient medium is small or occurs slowly, the large-scale structure of the plasma tails of comets appears to be robust to a disruptive change.

We expect that the average speed measurements shown in Figures 3 and 4 have a random error of $\pm 10 \text{ km s}^{-1}$ for Encke

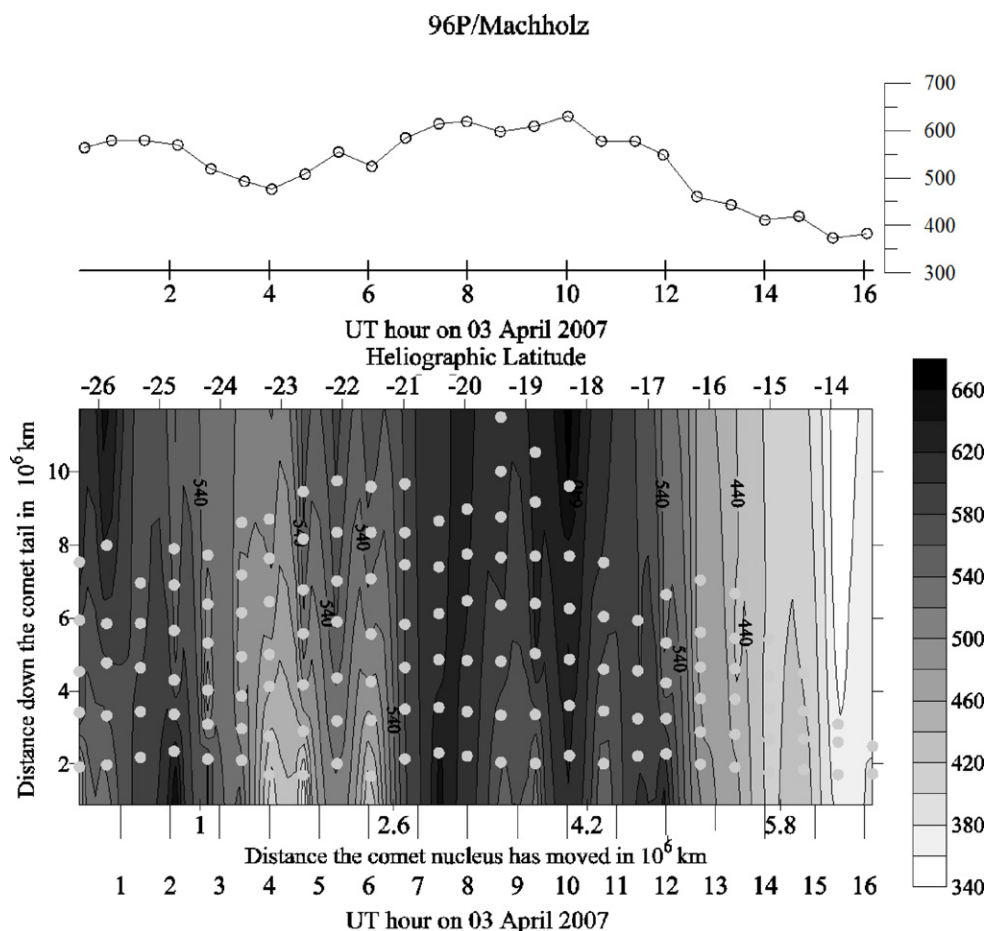


Figure 4. Radial velocity measurements of comet 96P/Machholz. Bottom: velocity contours in km s^{-1} , beginning 2007 April 3 at 00:10 UT, using measurements from HI-1A images. Top: average speed in km s^{-1} of each vertical column of radial measurements in the bottom panel.

and $\pm 13 \text{ km s}^{-1}$ for Machholz and that the errors in each speed measurement at 40 minute intervals are uncorrelated. The errors are determined by an estimation of the measurement uncertainty in locating each plasma crossing point, and then transferring this to a radial position error down the tail. These analyses show that solar wind velocities at the distances from the Sun of comets Machholz ($\sim 0.15 \text{ AU}$) and Encke ($\sim 0.34 \text{ AU}$) near perihelion were highly variable, ranging from 350 km s^{-1} to 670 km s^{-1} and from 200 km s^{-1} to 580 km s^{-1} , respectively.

In these measurements, the variations in speed for comet Encke are seen to be primarily associated with the ICME on 2007 April 20; this caused an abrupt change (Figure 3) beginning at about 14:50 UT and increasing until 16:50 UT, when the bright ICME front appears to engulf the comet and the complete disconnection becomes apparent. We associate this steady increase in solar wind speed from the ambient value of 300 km s^{-1} , up to 500 km s^{-1} , with the passage of the bright ICME front just prior to the disconnection.

We speculate, as have Vourlidis et al. 2007, that the sudden-transient nature of the bright portion of the ICME impacting Encke is undoubtedly associated with the disconnection of the comet tail. This front is associated with our measurements of a sustained higher solar wind speed. This higher speed and more dense portion of the CME likely carries with it an enhanced magnetic field, and is almost certainly responsible for the disconnection of the comet tail (Jia et al. 2009). An abrupt 200 km s^{-1} spike in solar wind speed above the ambient precedes the CME brightness enhancement by about 6 hr, and

this is most likely an indication of a fast shock that precedes the ICME into the interplanetary medium.

We thank C. Eyles of the University of Birmingham, UK, for SECCHI HI data and J. Davies of the Rutherford Appleton Laboratory (RAL), UK for help with HI image processing. This work was supported in part by grants NASA NNX08AJ11G and NSF ATM0852246, and one of us (M.M.B.) by NSF ATM 0925023.

REFERENCES

- Biermann, L. 1951, *Zh. Fiz. Astrophys.*, **29**, 274
 Buffington, A., Bisi, M. M., Clover, J. M., Hick, P. P., Jackson, B. V., & Kuchar, T. A. 2008, *ApJ*, **677**, 798
 Eyles, C. J., et al. 2003, *Sol. Phys.*, **217**, 319
 Eyles, C. J., et al. 2009, *Sol. Phys.*, **254**, 387
 Hick, P. P., Buffington, A., & Jackson, B. V. 2007, *Proc. SPIE*, **6689**, 66890C
 Howard, R. A., Moses, J. D., Socker, D. G., & the SECCHI Consortium 2000, *Proc. SPIE*, **4139**, 259
 Howard, R. A., et al. 2008, *Space Sci. Rev.*, **136**, 67
 Jackson, B. V., et al. 2004, *Sol. Phys.*, **225**, 177
 Jia, Y. D., et al. 2009, *ApJ*, **696**, L56
 Kaiser, M. L. 2005, *Adv. Space Res.*, **36**, 1483
 Kaiser, M. L., Kucera, T. A., Davila, J. M., St. Cyr, O. C., Guhathakurta, M., & Christian, E. 2008, *Space Sci. Rev.*, **136**, 5
 Kuchar, T. A., et al. 2008, *J. Geophys. Res.*, **113**, A04101
 Parker, E. N. 1958, *ApJ*, **128**, 664
 Socker, D. G., Howard, R. A., Korendyke, C. M., Simnett, G. M., & Webb, D. F. 2000, *Proc. SPIE*, **4139**, 284
 Vourlidis, A., Davis, C. J., Eyles, C. J., Crothers, S. R., Harrison, R. A., Howard, R. A., Moses, J. D., & Socker, D. G. 2007, *ApJ*, **668**, L79